DOPAMINE STIMULATES SALIVARY DUCT CELLS IN THE COCKROACH *PERIPLANETA AMERICANA*

INGO LANG* AND BERND WALZ

Department of Zoophysiology and Cell Biology, University of Potsdam, Lennéstraße 7a, 14471 Potsdam, Germany

*e-mail: ilang@rz.uni-potsdam.de

Summary

This study examines whether the salivary duct cells of the cockroach *Periplaneta americana* can be stimulated by the neurotransmitters dopamine and serotonin. We have carried out digital Ca^{2+}-imaging experiments using the Ca^{2+}-sensitive dye fura-2 and conventional intracellular recordings from isolated salivary glands. Dopamine evokes a slow, almost tonic, and reversible dose-dependent elevation in $[Ca^{2+}]_i$ in the duct cells. Upon stimulation with 10^{-6} mol l^{-1} dopamine, $[Ca^{2+}]_i$ rises from 48 ± 4 nmol l^{-1} to 311 ± 43 nmol l^{-1} (mean ± S.E.M., $N=18$) within 200–300 s. The dopamine-induced elevation in $[Ca^{2+}]_i$ is absent in Ca^{2+}-free saline and is blocked by 10^{-4} mol l^{-1} La^{3+}, indicating that dopamine induces an influx of Ca^{2+} across the basolateral membrane of the duct cells. Stimulation with 10^{-6} mol l^{-1} dopamine causes the basolateral membrane to depolarize from -67 ± 1 to -41 ± 2 mV ($N=10$). This depolarization is also blocked by La^{3+} and is abolished when Na$^+$ in the bath solution is reduced to 10 mmol l^{-1}. Serotonin affects neither $[Ca^{2+}]_i$ nor the basolateral membrane potential of the duct cells. These data indicate that the neurotransmitter dopamine, which has previously been shown to stimulate fluid secretion from the glands, also stimulates the salivary duct cells, suggesting that dopamine controls their most probable function, the modification of primary saliva.

Key words: calcium, cockroach, *Periplaneta americana*, duct, insect, salivary gland, serotonin.

Introduction

Insects have either morphologically simple tubular or very complex innervated acinar salivary glands. Among the acinar glands, the structure, innervation and several aspects of the aminergic control of salivation have been extensively studied in cockroaches and locusts (for reviews, see Ali, 1997; House and Ginsborg, 1985). Nevertheless, we are far from understanding the complex physiology of salivation with respect to acinar salivary glands. The key cellular mechanisms of saliva production, the mechanisms that contribute to the modification of the primary saliva and the neural control of all cell types engaged in saliva production are not known.

The secretory acini in the salivary glands of the cockroach *Periplaneta americana* contain two morphologically and functionally distinct cell types: a pair of peripheral cells and eight central cells. The peripheral cells are specialized for electrolyte/water transport, and the central cells for the production and secretion of proteins and mucins (Just and Walz, 1994a–c; Kessel and Beams, 1963). The glands are innervated from the suboesophageal ganglion, the stomatogastric nervous system and the satellite nervous system (Elia et al., 1994; Davis, 1985; Whitehead, 1971), and the biogenic amines dopamine and serotonin have been identified as neurotransmitters stimulating salivation (Evans and Green, 1991; Smith and House, 1979; Whitehead, 1973; for a review,

see House and Ginsborg, 1985). We have recently shown that dopamine stimulates the production of a completely protein-free, watery saliva, whereas serotonin is necessary to stimulate secretion of the proteinaceous saliva components (Just and Walz, 1996). Thus, dopamine is not merely more effective in stimulating salivation than serotonin: dopamine and serotonin stimulate different cell types.

Several lines of evidence suggest that the primary saliva is modified by the salivary duct epithelial cells. *In situ* electron-probe X-ray microanalysis of cryosections through *P. americana* salivary glands suggests (1) that the acini produce a NaCl-rich primary saliva and (2) that the primary saliva is modified within the ducts by Na$^+$ reabsorption and K$^+$ secretion (Gupta and Hall, 1983). The distal duct cells have all the ultrastructural characteristics of epithelial cells engaged in transport functions. Both their apical and basolateral plasma membrane domains are enlarged by deep infoldings, and they contain many mitochondria (Just and Walz, 1994a). Immunocytochemical investigations have shown that the basolateral plasma membrane domain is rich in Na$^+$/K$^+$-ATPase, whereas the apical plasma membrane domain is equipped with a vacuolar-type proton pump (V-H$^+$-ATPase; Just and Walz, 1994b). In addition, the salivary duct epithelial cells contain carbonic anhydrase, the enzyme responsible for

the reversible hydration of CO_2 (Just and Walz, 1994c). In spite of these findings, the mechanisms by which the salivary ducts modify the primary saliva are unknown. It is also unclear whether the activity of the salivary duct epithelial cells is influenced by the closely juxtaposed salivary duct nerve or neurotransmitter(s) in the haemolymph. Indeed, Whitehead (1971) has demonstrated that branches of the salivary duct nerve form a plexus on the ducts in *P. americana* and, more recently, Bräunig (1997) has shown that the octopaminergic DUM1B neurones form dense neurohaemal networks on salivary gland nerves in *Locusta migratoria*.

The immediate aim of the present work was to investigate whether the salivary duct epithelial cells in *P. americana* are stimulated by the neurotransmitters dopamine and/or serotonin. Conventional intracellular recordings and Ca^{2+}-imaging experiments have therefore been used to study the effects of dopamine and serotonin on salivary duct cells.

Materials and methods
Animals and preparations

A colony of *Periplaneta americana* (Blattodea, Blattidae) was reared at 27 °C under a 12 h:12 h L:D regime. The animals had free access to food and water. Imagines of both sexes were used.

The salivary glands were dissected from the animals in oxygenated cockroach physiological saline as described previously (Just and Walz, 1994a). Small pieces of the salivary glands, consisting of one lobe with its acini and duct system, were examined.

Solutions

The cockroach physiological saline had the following composition (in mmol l^{-1}): 160 NaCl, 10 KCl, 2 CaCl$_2$, 2 MgCl$_2$, 10 glucose, 10 Tris. The pH was adjusted with HCl to 7.4. The nominally Ca^{2+}-free solution contained no added CaCl$_2$ and 1 mmol l^{-1} EGTA. All solutions were continuously gassed with oxygen. Osmolarity was checked using an automatic osmometer (Knauer, Berlin, Germany) and was 355 mosmol l^{-1}. The Ca^{2+}-free solution had a slightly lower osmolarity since it contained EGTA, and less HCl was required to adjust the pH. To avoid osmotic gradients and cell swelling, this difference was corrected using mannitol.

A 10^{-2} mol l^{-1} dopamine stock solution was stored in aliquots of 200 μl at −20 °C, which were diluted in physiological saline immediately before an experiment. Oxygen was passed through the dopamine-containing solutions only while the solution was actually being used. Dopamine-containing solutions were replaced by fresh solution after 10 min of oxygenation.

Fura-2 AM was obtained from Molecular Probes (Eugene, OR, USA), and dopamine and serotonin were obtained from Sigma (Deisenhofen, Germany). All other chemicals were of analytical grade and were obtained from various suppliers.

Ca^{2+}-imaging

Ca^{2+}-imaging experiments were performed as described

previously (Zimmermann and Walz, 1997). Isolated lobes of the salivary glands were loaded with fura-2 at room temperature (20–22 °C) by a 15 min incubation in 5 μmol l^{-1} fura-2 AM in physiological saline. The lobes were then mounted in a rhomboid recording chamber (Science Products, Hofheim, Germany) and continuously superfused with oxygenated physiological saline. The coverslip-bottom of the chamber was coated with Cell-Tak tissue adhesive (Collaborative Biomedical Products, Bedford, USA) and changed after every experiment.

The chamber was mounted on a Zeiss Axiovert 135TV inverted microscope equipped with epifluorescence optics and a Zeiss Fluar 20 (numerical aperture 0.75) objective. Epifluorescent excitation was produced by a 75 W xenon arc lamp monochromator unit connected to the microscope by a quartz fibre-optic light guide. The epifluorescence filter-block in the microscope contained a 450 nm dichroic mirror and a 515–565 nm bandpass emission filter. Pairs of fluorescence images were excited at 340 and 380 nm and captured and digitized with a cooled image transfer CCD camera (TE/CCD-512EFT, Princeton Instruments Corp., Trenton, NJ, USA) at a rate of 0.5–0.2 s^{-1} at 12-bit resolution. A 5×5 binning application to individual pixels resulted in a spatial resolution of 3.8 μm. Monochromator control, image acquisition and processing were carried out using the imaging software Metafluor 2.75 (Universal Imaging Corp., PA, USA) on a personal computer.

The free Ca^{2+} concentration ([Ca^{2+}]$_{free}$) was calculated in the 340 nm and 380 nm image pairs using the equation (Grynkiewicz et al., 1985):

$$[Ca^{2+}]_{free} = K_D[(R - R_{min})/(R_{max} - R)](F_{380,max}/F_{380,min}),$$

where, K_D is the dissociation constant, R is the ratio of each 340 nm/380 nm pixel pair, R_{min} and R_{max} are the ratios at saturating and zero Ca^{2+} concentrations, respectively, and $F_{380,max}$ and $F_{380,min}$ are the maximal and minimal fluorescence intensities at 380 nm at saturating and zero Ca^{2+} concentrations, respectively. These variables were measured *in vitro* using a Ca^{2+} calibration kit (Molecular Probes, Eugene, OR, USA) and were as follows: K_D=205.7±10.2 nmol l^{-1}, R_{min}=0.41±0.01, R_{max}=3.29±0.15 and $F_{380,max}/F_{380,min}$=3.75±0.24 (means ± S.E.M, N=6). Before quantification, cell autofluorescence was determined at the end of each experiment by quenching the fura-2 fluorescence with 20 mmol l^{-1} Mn^{2+} and subtracting the autofluorescence from each image. Quantitative data on [Ca^{2+}]$_i$ were obtained by integrating the signals over a region measuring 19 μm×19 μm.

Electrical measurements

Lobes of the salivary glands were mounted in the recording chamber as described above and continuously superfused with oxygenated physiological saline at a flow rate of 1.2 ml min^{-1}. Conventional microelectrodes were filled with 3 mol l^{-1} KCl and had resistances of approximately 80 MΩ. Salivary duct cells were impaled *via* the basolateral membrane under optical control (Leica DM IBB inverted microscope). Potential

differences were measured using an L/M-PC amplifier (List-Medical, Darmstadt, Germany) in current-clamp mode, monitored on an oscilloscope and stored on a personal computer using the software Chart 8.11 (HEKA, Lambrecht/Pfalz, Germany).

In some experiments, intracellular recordings and Ca^{2+}-imaging were performed simultaneously on the imaging setup using a Bramp 01 amplifier (npi, Tamm, Germany) for intracellular recordings.

Statistics

Values are expressed as arithmetic means ± S.E.M. Results were compared statistically using a paired Student's *t*-test. *P* values of less than 0.05 were considered significant. Graphs were plotted using SigmaPlot 4.0 (Jandel Scientific, San Rafael, CA, USA). Figures that show values from a single experiment are representative of at least three independent experiments. Only one region per imaging experiment was used for quantitative analysis.

Results

Effects of dopamine and serotonin on cytoplasmic Ca^{2+} concentration

In the unstimulated salivary duct cells, the intracellular free Ca^{2+} concentration ($[Ca^{2+}]_i$) was $48 \pm 4\,\mathrm{nmol\,l^{-1}}$ (N=18). Serotonin concentrations up to $10\,\mathrm{\mu mol\,l^{-1}}$ had no effect on $[Ca^{2+}]_i$, whereas stimulation with $1\,\mathrm{\mu mol\,l^{-1}}$ dopamine induced a reversible, slow rise in $[Ca^{2+}]_i$. The elevation in $[Ca^{2+}]_i$ began 20–140 s after the addition of dopamine and reached $311 \pm 43\,\mathrm{nmol\,l^{-1}}$ (N=18) (Fig. 1). In some preparations, the dopamine-induced increase in $[Ca^{2+}]_i$ was preceded by an initial small brief fall in $[Ca^{2+}]_i$ (see Figs 3, 5, 6, 7A). The
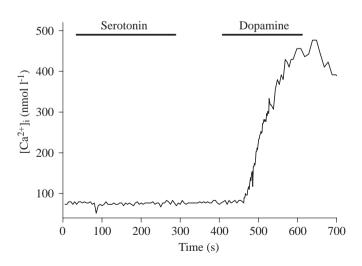

Fig. 1. Effects of $10\,\mathrm{\mu mol\,l^{-1}}$ serotonin and $1\,\mathrm{\mu mol\,l^{-1}}$ dopamine on $[Ca^{2+}]_i$ in a salivary duct cell. Serotonin has no effect on $[Ca^{2+}]_i$, whereas dopamine causes, after a delay of approximately 55 s, a slow elevation in $[Ca^{2+}]_i$. After the application of serotonin, the preparation was washed with saline for 100 s before exposure to dopamine.
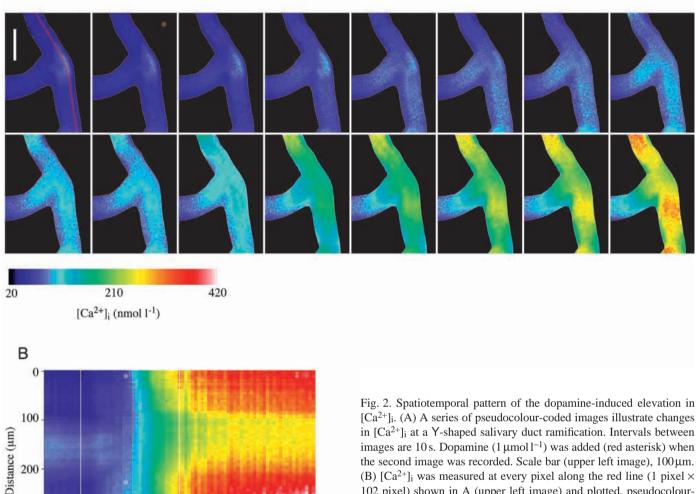
dopamine-induced elevation in $[Ca^{2+}]_i$ was almost tonic (see Fig. 4) or declined slowly after reaching its peak value in the continuous presence of dopamine (see Figs 5, 11A). The spatiotemporal pattern of the dopamine-induced elevation in $[Ca^{2+}]_i$ is illustrated in the series of pseudocolour images in Fig. 2A. To evaluate the spatiotemporal $[Ca^{2+}]_i$ dynamics, we defined a line (1 pixel wide, 102 pixels long) in the sequence of background-subtracted images, calculated $[Ca^{2+}]_i$ in each pixel along the line, and translated $[Ca^{2+}]_i$ into pseudocolour values. These were plotted as a space–time plot, where distance was the ordinate and time the abscissa (Fig. 2B). This space–time plot shows that $[Ca^{2+}]_i$ starts increasing at several points in the duct epithelium and, from there, the increase in $[Ca^{2+}]_i$ seems to spread slowly over the duct. Not all regions of the duct seem to reach the maximum $[Ca^{2+}]_i$. It is interesting to note that, in contrast to the rise in $[Ca^{2+}]_i$, the initial brief fall in $[Ca^{2+}]_i$ described above occurs at the same time in all parts of the duct epithelium (Fig. 3). The velocity at which the elevation in $[Ca^{2+}]_i$ spreads over the ducts was estimated by fitting a straight line along regions with similar colour, as illustrated in Fig. 3. The velocity of this Ca^{2+} 'tide', which is represented by the slope of the line, is $3.7 \pm 0.6\,\mathrm{\mu m\,s^{-1}}$ (N=4).

The dopamine-induced elevation in $[Ca^{2+}]_i$ is dose-dependent and, particularly at lower concentrations, almost tonic (Fig. 4A,B). Another characteristic feature of the dopamine-induced elevation in $[Ca^{2+}]_i$ is that its size depends on the history of stimulation. When the duct cells are stimulated twice with $1\,\mathrm{\mu mol\,l^{-1}}$ dopamine, the second dopamine application causes an elevation in $[Ca^{2+}]_i$ to a concentration 4.2 ± 1.4 times larger than that for the first stimulation (N=4) (Fig. 5).

To test whether the dopamine-induced increase in $[Ca^{2+}]_i$ is attributable to Ca^{2+} release from intracellular stores or to Ca^{2+} influx from the extracellular space, we applied $1\,\mathrm{\mu mol\,l^{-1}}$ dopamine in a nominally Ca^{2+}-free physiological saline. Superfusion of the preparation with Ca^{2+}-free saline did not affect the baseline cytoplasmic Ca^{2+} concentration (Fig. 6A). However, under Ca^{2+}-free conditions, no elevation in $[Ca^{2+}]_i$ could be observed upon stimulation with dopamine. Subsequent superfusion with normal Ca^{2+}-containing physiological saline restored the ability of the duct cells to produce an increase in $[Ca^{2+}]_i$ upon stimulation with dopamine. The results of six independent experiments, such as that illustrated in Fig. 6A, are summarized in Fig. 6B. The slightly higher $[Ca^{2+}]_i$ under Ca^{2+}-free conditions in the presence of $1\,\mathrm{\mu mol\,l^{-1}}$ dopamine is attributable to the finding that, after the first control stimulation with dopamine, $[Ca^{2+}]_i$ returned only very slowly to its pre-stimulus baseline concentration. These experiments show that the dopamine-induced elevation in $[Ca^{2+}]_i$ is completely attributable to Ca^{2+} influx across the basolateral plasma membrane of the duct cells.

In many systems, stimulus-induced Ca^{2+} entry into cells is blocked by La^{3+}. The experiment illustrated in Fig. 7A shows that, in the presence of $100\,\mathrm{\mu mol\,l^{-1}}$ La^{3+}, dopamine fails to stimulate an elevation in $[Ca^{2+}]_i$. The La^{3+} block is almost

A

B

Fig. 2. Spatiotemporal pattern of the dopamine-induced elevation in $[Ca^{2+}]_i$. (A) A series of pseudocolour-coded images illustrate changes in $[Ca^{2+}]_i$ at a Y-shaped salivary duct ramification. Intervals between images are 10 s. Dopamine ($1 \mu mol\, l^{-1}$) was added (red asterisk) when the second image was recorded. Scale bar (upper left image), $100 \mu m$. (B) $[Ca^{2+}]_i$ was measured at every pixel along the red line (1 pixel × 102 pixel) shown in A (upper left image) and plotted, pseudocolour-coded, in a space–time plot. The time of dopamine addition is marked by a red arrow. The times at which the first and last image in A were taken are labelled as vertical white lines. $[Ca^{2+}]_i$ begins to rise at several sites (white asterisks) and then the increase in $[Ca^{2+}]_i$ appears to spread out slowly over the duct system. The pseudocolour bar below A represents $[Ca^{2+}]_i$ in A and B.

irreversible, and no second stimulation could be obtained with dopamine after washing out the La^{3+}. The results from five La^{3+} experiments are summarized in Fig. 7B.

To characterize further the dopamine-induced increase in $[Ca^{2+}]_i$, we tested whether it was mediated by a voltage-sensitive Ca^{2+} entry pathway. For this purpose, we superfused the preparation with a physiological saline in which $[K^+]$ was elevated to $100\, mmol\, l^{-1}$ ($[Na^+]$ was reduced to $70\, mmol\, l^{-1}$). This high-K^+ medium depolarized the cells by $49\pm1.0\, mV$ ($N=5$); $[Ca^{2+}]_i$, however, was unaffected by this depolarization (results not shown).

Effects of dopamine and serotonin on basolateral membrane potential

Unstimulated salivary duct cells had basolateral membrane potentials, PD_b, of $-67\pm0.9\, mV$ ($N=10$). Serotonin had no effect on PD_b at concentrations up to $10\, \mu mol\, l^{-1}$ (results not

shown), while $1\, \mu mol\, l^{-1}$ dopamine produced a slowly rising and long-lasting depolarization of PD_b to $41\pm2.3\, mV$ ($N=10$) (Fig. 8).

We tested whether the dopamine-induced depolarization of the duct cells was Na^+-dependent. For this purpose, we superfused the preparation with a physiological solution in which $[Na^+]$ was reduced to $10\, mmol\, l^{-1}$ by substituting $150\, mmol\, l^{-1}$ N-methyl-D-glucamine (NMDG) for Na^+. Superfusion of the preparation with this low-Na^+ medium produced a small liquid junction potential of several millivolts (Fig. 9). Addition of $1\, \mu mol\, l^{-1}$ dopamine to the low-Na^+ saline produced no depolarization. The dopamine-induced depolarization developed reversibly, however, when the normal extracellular Na^+ concentration was re-established in the continuous presence of dopamine (Fig. 9). Thus, the dopamine-induced depolarization requires a high Na^+ concentration on the basolateral side of the salivary ducts. It
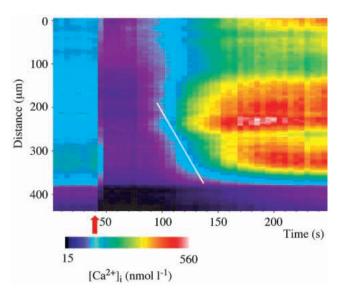
Fig. 3. Example of a space–time plot generated from a line (1 pixel × 114 pixel) on the duct system. The brief drop in the Ca^{2+} signal that precedes the increase in $[Ca^{2+}]_i$ occurs at the same time in all parts of the duct. In contrast, the subsequent increase in $[Ca^{2+}]_i$ spreads out slowly over the duct. In the part of the duct epithelium represented in the lower area of the graph, $[Ca^{2+}]_i$ barely rises after the initial fall in $[Ca^{2+}]_i$. The slope of the white line fitted along pixels with the same colour represents the velocity of the Ca^{2+} 'tide'. The time of dopamine addition (10^{-6} mol l^{-1}) is marked by a red arrow. The pseudocolour bar below represents $[Ca^{2+}]_i$.

should be mentioned that dopamine, although it did not depolarize the duct cells in low-Na⁺ saline, did elevate $[Ca^{2+}]_i$ under these conditions (results not shown).

We next tested whether 100 μmol l^{-1} La^{3+}, which blocks the dopamine-induced elevation in $[Ca^{2+}]_i$, also affects the depolarization induced by dopamine. La^{3+} blocked the depolarization almost completely. The remaining depolarization was only 14±1.8 % (*N*=3) of the control depolarization and was transient (results not shown).

Simultaneous intracellular electrical recordings and Ca²⁺ measurements

We attempted to correlate the kinetics of the dopamine-induced depolarizations and changes in $[Ca^{2+}]_i$ by simultaneous intracellular electrical recordings and Ca^{2+}-imaging. In these experiments, the microelectrode tip was localized using differential interference contrast optics, and the region of interest for localized Ca^{2+} measurements was positioned in the fluorescent Ca^{2+} images over the tip of the microelectrode (Fig. 10). The result of such a simultaneous $[Ca^{2+}]_i$ and electrical recording is shown in Fig. 11A, together with the raw fluorescence at 340 and 380 nm excitation in Fig. 11B. The first 300 s of this experiment at a higher time resolution are demonstrated in Fig. 11C, during which the time points A–F mark the times when the Ca^{2+} images in Fig. 10A–F were recorded. A comparison of the $[Ca^{2+}]_i$ trace and the PD_b trace in Fig. 11A and Fig. 11C shows (1) that the

onset of the elevation in $[Ca^{2+}]_i$ seems to lag behind the onset of the depolarization by approximately 90 s, (2) that, after this delay, $[Ca^{2+}]_i$ rises faster than the depolarization, (3) that $[Ca^{2+}]_i$ starts to decrease in the presence of dopamine, whereas the cell is still depolarizing slowly, (4) that, after the dopamine has been washed out, $[Ca^{2+}]_i$ recovers monotonically to baseline values, whereas PD_b starts to recover only after a delay of approximately 100 s but then decreases faster than $[Ca^{2+}]_i$. In three further identical experiments, the time differences between the onset of the dopamine-induced depolarization and the increase in $[Ca^{2+}]_i$ were 20, 60 and 90 s. The membrane potential always rose earlier than $[Ca^{2+}]_i$. In some experiments (Fig. 12A,B), the often observed initial decrease in $[Ca^{2+}]_i$ after dopamine stimulation started simultaneously with the depolarization.

To understand the time delay between the electrical response and the change in $[Ca^{2+}]_i$, it is necessary to inspect the raw traces of the fluorescence measured at 340 and 380 nm
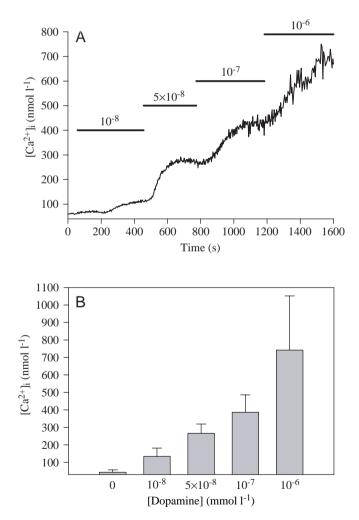

Fig. 4. Concentration-dependence of dopamine-induced intracellular elevations in $[Ca^{2+}]_i$. (A) Original recording showing elevations in $[Ca^{2+}]_i$ induced by 10, 50 and 100 nmol l^{-1} and 1 μmol l^{-1} dopamine. The dopamine-induced elevations in $[Ca^{2+}]_i$ are almost tonic. (B) Quantitative analysis of five independent experiments such as that illustrated in A. Values are means + S.E.M.
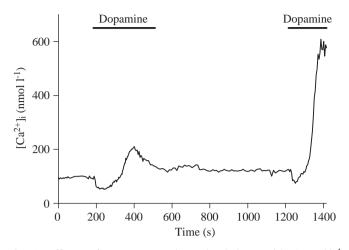
Fig. 5. Effects of two consecutive stimulations with $1\,\mu mol\,l^{-1}$ dopamine, showing that the size of the dopamine-induced elevation in $[Ca^{2+}]_i$ depends on the history of stimulation. When the duct cells are stimulated twice, the second increase in $[Ca^{2+}]_i$ is larger than the first. This recording also shows that, after dopamine application, there may be a brief reduction in the Ca^{2+} signal before $[Ca^{2+}]_i$ starts to increase.

excitation (Fig. 11B) and to keep in mind that an increase in $[Ca^{2+}]_i$ causes antiparallel changes in the 340 and 380 nm signals: the fluorescence excited at 340 nm rises, whereas the fluorescence excited at 380 nm falls. A parallel rise or fall of both signals occurs when the dye concentration changes, e.g. through changes in cellular volume. At the onset of the depolarization, the fluorescent intensities excited at 340 and 380 nm fall faster than in the unstimulated duct (bleaching), whereas $[Ca^{2+}]_i$ appears to remain unchanged (Fig. 11A,B). Only when $[Ca^{2+}]_i$ starts rising, do the 340 and 380 nm signals change in an antiparallel way. The most likely explanation for the apparent delay in the onset of the elevation in $[Ca^{2+}]_i$ with respect to the depolarization is a dopamine-induced cell swelling, resulting in a decrease in the intracellular dye concentration. An increase in cell volume, not apparent in electrical recordings, could cancel a small initial Ca^{2+}-influx-induced elevation in $[Ca^{2+}]_i$ and delay the measurable increase in $[Ca^{2+}]_i$.

Discussion

The main finding of the present study is that the neurotransmitter dopamine, which has been shown to stimulate fluid secretion in the salivary glands of the cockroaches *Periplaneta americana* and *Nauphoeta cinerea* (Just and Walz, 1996; for a review, see House and Ginsborg, 1985), also stimulates the salivary gland duct cells downstream of the acini. This result suggests that the most likely function of the salivary gland duct cells, i.e. the modification of the primary saliva, is under the control of the same neurotransmitter that stimulates fluid secretion by the peripheral cells in the acini.

The most likely sources of the dopamine in intact animals are the axons of the paired SN1 neurones. These two neurones
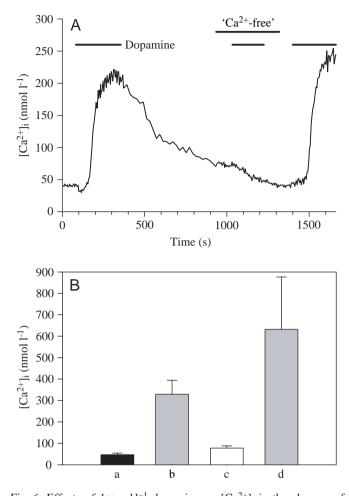

Fig. 6. Effects of $1\,\mu mol\,l^{-1}$ dopamine on $[Ca^{2+}]_i$ in the absence of extracellular Ca^{2+}. (A) After a control stimulation in normal physiological saline, the preparation was superfused with Ca^{2+}-free saline and again stimulated with dopamine. Under these conditions, dopamine elicits no elevation in $[Ca^{2+}]_i$. This effect is reversible as shown by a second control stimulation in normal saline. (B) Summary of six independent experiments such as that illustrated in A. a, unstimulated; b, $10^{-6}\,mol\,l^{-1}$ dopamine; c, $10^{-6}\,mol\,l^{-1}$ dopamine/'Ca^{2+}-free'; d, $10^{-6}\,mol\,l^{-1}$ dopamine, second control stimulation. The experiments demonstrate that the rise in $[Ca^{2+}]_i$ is caused by Ca^{2+} influx from the extracellular space. Values are means + S.E.M.

are located in the suboesophageal ganglion and innervate the salivary glands *via* nerve 7b, i.e. the salivary nerve that projects to the glands by following the salivary ducts and is spatially closely juxtaposed to the ducts. The SN1 neurones are most probably dopaminergic, because their axons have been shown to have tyrosine-hydroxylase-like immunoreactivity (Elia et al., 1994; for a review and critical discussion, see Ali, 1997). With respect to a possible dopaminergic input from the salivary duct nerve to the duct cells, it is important to note that small tyroxine-hydroxylase-like immunoreactive neurohaemal processes are associated with the salivary ducts in *Carausius morosus* (Ali and Orchard, 1996). It has been proposed that these processes, which have not yet been described for either
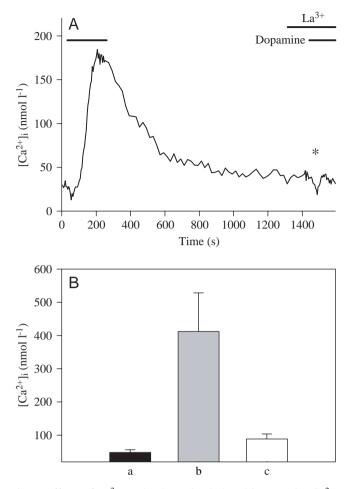
Fig. 8. Intracellular recording from a salivary duct cell showing that $1\,\mu mol\,l^{-1}$ dopamine induces a reversible depolarization of the basolateral cell membrane of almost $20\,mV$.

Fig. 7. Effects of La^{3+} on the dopamine-induced increase in $[Ca^{2+}]_i$. (A) La^{3+} ($100\,\mu mol\,l^{-1}$) completely blocks the dopamine-induced elevation in $[Ca^{2+}]_i$. The brief drop in the Ca^{2+} signal that precedes the increase in $[Ca^{2+}]_i$ in many preparations seems to be little affected by La^{3+} (*). (B) Quantitative analysis of the results from five independent experiments such as that illustrated in A. a, unstimulated; b, $10^{-6}\,mol\,l^{-1}$ dopamine; c, $10^{-6}\,mol\,l^{-1}$ dopamine/$10^{-4}\,mol\,l^{-1}$ La^{3+}.

P. americana or *L. migratoria*, activate the salivary duct cells to induce transport processes for the modification of the primary saliva. In this study, we have now been able to show directly that dopamine has at least two effects on the duct cells: a Na^+-dependent depolarization of the basolateral membrane that can be blocked by La^{3+}, and an increase in $[Ca^{2+}]_i$, which is absent in Ca^{2+}-free physiological saline and is also blocked by La^{3+}. The latter results indicate that the dopamine-induced elevation in $[Ca^{2+}]_i$ is due entirely to an influx of Ca^{2+} across the basolateral membrane.

The temporal pattern of the dopamine-induced elevation in $[Ca^{2+}]_i$ requires some attention. Agonist-induced Ca^{2+} signals in a large variety of cells have been shown to exhibit complex patterns: low agonist concentrations evoke periodic oscillations in $[Ca^{2+}]_i$ arising from cyclical Ca^{2+} release from, and reuptake into, the endoplasmic reticulum (and/or from Ca^{2+} movements across the plasma membrane), whereas high
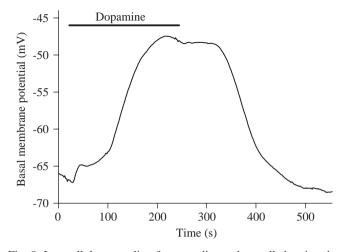
agonist concentrations cause biphasic elevations in $[Ca^{2+}]_i$ consisting of an initial transient followed by a sustained plateau (Berridge, 1993; Fewtrell, 1993). In *P. americana* salivary duct cells, dopamine causes slowly rising sustained elevations in $[Ca^{2+}]_i$. Thus, information about the agonist concentration is coded in the amplitude rather than the frequency of the Ca^{2+} signal. Such purely amplitude-modulated signalling is rare (Berridge, 1997). Among the few examples are Ca^{2+} signals in B lymphocytes (Dolmetsch et al., 1997) and invertebrate
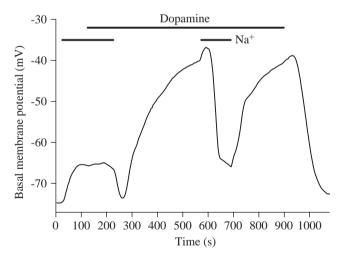

Fig. 9. Na^+-dependence of the dopamine-induced depolarization. The preparation was first superfused with a physiological saline containing only $10\,mmol\,l^{-1}$ Na^+ ($150\,mmol\,l^{-1}$ NMDG substituted for Na^+). This low-Na^+ saline produced a small depolarization (liquid junction potential). Subsequent addition of $1\,\mu mol\,l^{-1}$ dopamine did not depolarize the cell. In the continuous presence of dopamine, re-addition of Na^+ caused the cell, after a brief hyperpolarization, to depolarize by approximately $35\,mV$. When $[Na^+]$ was again reduced to $10\,mmol\,l^{-1}$ in the presence of dopamine, the cell, after a brief and small further depolarization, hyperpolarized once more until the normal Na^+ concentration was re-established.
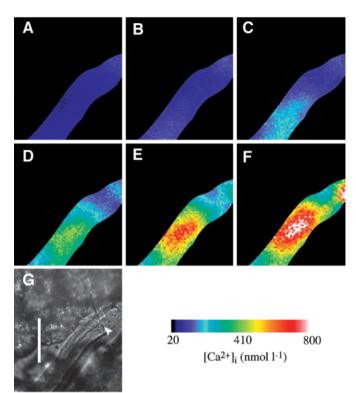
Fig. 10. Illustration of a Ca^{2+}-imaging experiment combined with a simultaneous intracellular recording of the membrane potential of a salivary duct cell. (G) A differential interference contrast micrograph of the salivary duct from which the Ca^{2+} images A–F were recorded. The tip of the recording electrode (white arrowhead) can also be seen. Scale bar, 100 μm. To obtain the fluorescence changes illustrated in Fig. 11, the region for quantitative analysis was placed over the microelectrode tip. The pseudocolour images A–F show the rise in $[Ca^{2+}]_i$ induced by 1 μmol l^{-1} dopamine. The times at which these images were acquired are labelled A–F in Fig. 11C.

microvillar photoreceptors (Levy and Fein, 1985; Walz et al., 1994). In the tubular salivary glands of the blowfly *Calliphora erythrocephala*, the neurohormone serotonin evokes intercellular $[Ca^{2+}]$ waves and intracellular $[Ca^{2+}]$ oscillations. The $[Ca^{2+}]$ waves propagate at rates of 12–17 μm s^{-1} (Zimmermann and Walz, 1997), which is approximately four times faster than the spreading Ca^{2+} 'tide' in the cockroach salivary ducts measured in the present study.

The depolarizing effect of dopamine on the salivary duct cells is diametrically opposite to the effects that dopamine exerts on cockroach salivary gland acinar cells. In the latter, dopamine has been shown to cause a Ca^{2+}-dependent hyperpolarization, possibly mediated by putative D_2-like receptors (Evans and Green, 1990, 1991; Gray et al., 1984; Ginsborg et al., 1980). This indicates that dopamine activates other, as yet unknown, transduction mechanisms in the duct cells.

We have tried to obtain information on whether both signals, i.e. the depolarization and the elevation in $[Ca^{2+}]_i$, follow the same time course and, thus, might be mediated by
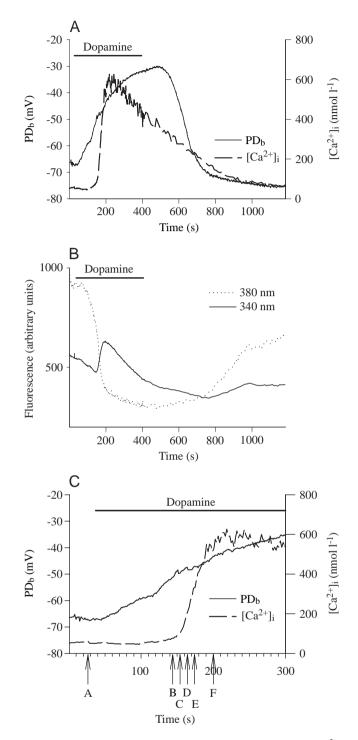

Fig. 11. Dopamine-induced depolarization and increase in $[Ca^{2+}]_i$ recorded simultaneously close to the tip of the recording microelectrode (same experiment as that illustrated in Fig. 10). (A) Electrophysiological recording of the basolateral membrane potential (PD_b) (continuous trace, left ordinate) and the change in $[Ca^{2+}]_i$ (broken trace, right ordinate). (B) Raw fluorescence signals recorded at excitation wavelengths of 340 and 380 nm. (C) Dopamine-induced depolarization and increase in $[Ca^{2+}]_i$ from A plotted at higher time resolution. The arrows labelled A–F indicate the times at which the pseudocolour images in Fig. 10 were acquired. Dopamine was added to give a final concentration of 10^{-6} mol l^{-1}.
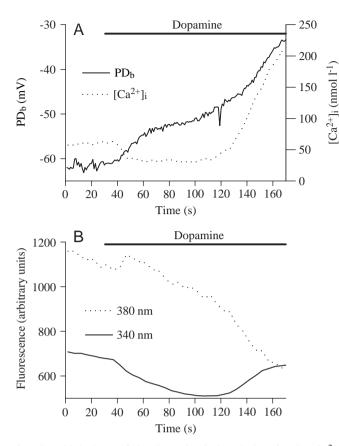
Fig. 12. Initial phase of the dopamine-induced elevation in $[Ca^{2+}]_i$ and depolarization recorded simultaneously. (A) Basolateral membrane potential (PD_b) (continuous trace, left ordinate) and $[Ca^{2+}]_i$ (dotted trace, right ordinate). (B) Raw fluorescence signals recorded at excitation wavelengths of 340 and 380 nm. Dopamine was added to give a final concentration of 10^{-6} mol l^{-1}.

depolarization and the Ca^{2+} influx are mediated by different mechanisms.

The luminal plasma membrane of the salivary duct cells in *P. americana* is equipped with a V-H^+-ATPase (Just and Walz, 1994b). In several insect ion-transporting epithelia, this proton pump is used to energize plasma membranes in order to drive secondary transport processes (Wieczorek et al., 1991; Klein, 1992). Little is known about the mechanisms that regulate apical proton pump molecules. An additional important subject for future studies will be whether V-H^+-ATPases can be regulated directly or indirectly by changes in $[Ca^{2+}]_i$.

References

Ali, D. W. (1997). The aminergic and peptidergic innervation of insect salivary glands. *J. Exp. Biol.* **200**, 1941–1949.

Ali, D. W. and Orchard, I. (1996). Immunohistochemical localization of tyrosine hydroxylase in the ventral cord of the stick insect, *Carausius morosus*, including neurons innervating the salivary glands. *Cell Tissue Res.* **285**, 453–462.

Berridge, M. J. (1993). Inositol trisphosphate and calcium signalling. *Nature* **361**, 315–325.

Berridge, M. J. (1997). The AM and FM of calcium signalling. *Nature* **386**, 759–760.

Bräunig, P. (1997). The peripheral branching pattern of identified dorsal unpaired median (DUM) neurones of the locust. *Cell Tissue Res.* **290**, 641–654.

Davis, N. T. (1985). Serotonin-immunoreactive visceral nerves and neurohemal system in the cockroach *Periplaneta americana* (L.). *Cell Tissue Res.* **240**, 593–600.

Dolmetsch, R. E., Lewis, R. S., Goodnow, C. C. and Healy, J. I. (1997). Differential activation of transcription factors induced by Ca^{2+} response amplitude and duration. *Nature* **386**, 855–858.

Elia, A. J., Ali, D. W. and Orchard, I. (1994). Immunochemical staining of tyrosine hydroxylase (TH)-like material in the salivary glands and ventral nerve cord of the cockroach, *Periplaneta americana* (L.). *J. Insect Physiol.* **40**, 671–683.

Evans, A. M. and Green, K. L. (1990). Characterization of the dopamine receptor mediating the hyperpolarization of cockroach salivary glands *in vitro*. *Br. J. Pharmac.* **101**, 103–108.

Evans, A. M. and Green, K. L. (1991). Effects of selective D_1 and D_2 dopamine agonists on cockroach salivary gland acinar cells *in vitro*. *Br. J. Pharmac.* **104**, 787–792.

Fewtrell, C. (1993). Ca^{2+} oscillations in non-excitable cells. *Annu. Rev. Physiol.* **55**, 427–454.

Ginsborg, B. L., House, C. R. and Mitchell, M. R. (1980). On the role of calcium in the electrical responses of cockroach salivary gland cells to dopamine. *J. Physiol., Lond.* **303**, 325–335.

Gray, D. C., Ginsborg, B. L. and House, C. R. (1984). Cyclic AMP as a possible mediator of dopamine stimulation of cockroach gland cells. *Q. J. Exp. Physiol.* **69**, 171–186.

Grynkiewicz, G., Poenie, M. and Tsien, R. Y. (1985). A new generation of Ca^{2+} indicators with greatly improved fluorescence properties. *J. Biol. Chem.* **260**, 3440–3450.

Gupta, B. L. and Hall, T. A. (1983). Ionic distribution in dopamine-

the same mechanisms or by functionally closely linked mechanisms. At first sight, the elevation in $[Ca^{2+}]_i$ seems to lag behind the onset of the depolarizing response by 20–90 s. A comparison of the two signals is complicated by the observation that, in some preparations, the elevation in $[Ca^{2+}]_i$ is preceded by a brief drop in $[Ca^{2+}]_i$ and that the latter starts simultaneously with the depolarization. Close inspection of the raw fluorescence signals, however, indicates that dopamine most probably induces an increase in volume of the duct cells; this might mask a small initial Ca^{2+}-influx-induced increase in $[Ca^{2+}]_i$. Activation of voltage-gated Ca^{2+} channels by the depolarization seems unlikely, because an elevation of the K^+ concentration in the superfusate to 100 mmol l^{-1} depolarizes the duct cells but produces no increase in $[Ca^{2+}]_i$ (results not shown). The definitive explanation of the mechanistic basis of the depolarization and the elevation in $[Ca^{2+}]_i$ warrants further experiments to address these questions specifically. The observation, however, that dopamine does not depolarize the duct cells but elevates $[Ca^{2+}]_i$ in low-Na^+ saline together with the gross differences in the time courses of the two signals suggest that the

stimulated NaCl fluid-secreting cockroach salivary glands. *Am. J. Physiol.* **244**, R176–R186.

House, C. R. and Ginsborg, B. L. (1985). Salivary gland. In *Comprehensive Insect Physiology and Pharmacology*, vol. 11 (ed. G. A. Kerkut and L. I. Gilbert), pp. 195–224. Oxford: Pergamon Press

Just, F. and Walz, B. (1994a). Salivary glands of the cockroach, *Periplaneta americana*: New data from light and electron microscopy. *J. Morph.* **220**, 35–46.

Just, F. and Walz, B. (1994b). Immunocytochemical localization of Na/K-ATPase and V-H-ATPase in the salivary gland of the cockroach, *Periplaneta americana*. *Cell Tissue Res.* **278**, 161–170.

Just, F. and Walz, B. (1994c). Localization of carbonic anhydrase in the salivary glands of the cockroach, *Periplaneta americana*. *Histochemistry* **102**, 271–277.

Just, F. and Walz, B. (1996). The effects of serotonin and dopamine on salivary secretion by isolated cockroach salivary glands. *J. Exp. Biol.* **199**, 407–413.

Kessel, R. G. and Beams, H. W. (1963). Electron microscope observations on the salivary gland of the cockroach, *Periplaneta americana*. *Z. Zellforsch. Mikrosk. Anat.* **59**, 857–877.

Klein, U. (1992). The insect V-ATPase, a plasma membrane proton pump energizing secondary active transport: immunological evidence for the occurence of a V-ATPase in insect ion-transporting epithelia. *J. Exp. Biol.* **172**, 345–354.

Levy, S. and Fein, A. (1985). Relationship between light sensitivity and intracellular free Ca concentration in *Limulus* ventral photoreceptors. A quantitative study using Ca-selective microelectrodes. *J. Gen. Physiol.* **85**, 805–841.

Smith, R. K. and House, C. R. (1979). Ion and water transport by isolated cockroach salivary glands. *J. Membr. Biol.* **51**, 325–346.

Walz, B., Zimmermann, B. and Seidl, S. (1994). Intracellular Ca^{2+} concentration and latency of light-induced Ca^{2+} changes in photoreceptors of the honey bee drone. *J. Comp. Physiol.* A **174**, 421–431.

Whitehead, A. T. (1971). The innervation of the salivary gland in the American cockroach: Light and electron microscopic observations. *J. Morph.* **135**, 483–506.

Whitehead, A. T. (1973). Innervation of the American cockroach salivary gland: Neurophysiological and pharmacological investigations. *J. Insect Physiol.* **19**, 1961–1970.

Wieczorek, H., Putzenlechner, M., Zeiske, W. and Klein, U. (1991). A vacuolar-type proton pump energizes K^+/H^+ antiport in an animal plasma membrane. *J. Biol. Chem.* **266**, 15340–15347.

Zimmermann, B. and Walz, B. (1997). Serotonin-induced intercellular calcium waves in salivary glands of the blowfly *Calliphora erythrocephala*. *J. Physiol., Lond.* **500**, 17–28.